JOURNAL OF MATERIALS SCIENCE **36** (2001) 511–518

A model for the evaluation of indentation crack arrest fracture toughness of supported films

B. BOZZINI
INFM-Dipartimento di Ingegneria dell'Innovazione, Università di Lecce, v. Arnesano, I-73100 Lecce, Italy
E-mail: bozzii@axpmzt.unile.it

M. BONIARDI
Dipartimento di Meccanica, Politecnico di Milano, pz. L. da Vinci 32, 20133 Milano, Italy

A simple model is proposed for the evaluation of crack-arrest fracture toughness K_{Ic0} of thin films by Vickers indentation. This approach applies to films thinner than the penetration depth of the Vickers indenter. The model equations are provided in closed form, even though they are so complex that they must be integrated numerically in practical applications. The problem of the evaluation of K_{Ic0} for thin films and substrates is derived in general form and applied to three cases: (i) evaluation of K_{Ic0} for the film in the case that the depth of the crack in the film is smaller than the film thickness, (ii) evaluation of K_{Ic0} for the film in the case that the crack emanating from the film either crosses the film/substrate interface or is stopped by it, (iii) evaluation of K_{Ic0} for the substrate in the case that the crack emanating from the film crosses the film/substrate interface. The model was tested with original and literature experimental data: (i) published K_{Ic0} values of electroless Ni-P thin films were re-evaluated, (ii) K_{Ic0} of electroless Ni-P thin films of various thickness with various loads were measured (original data) and computed, (iii) K_{Ic0} of electroless Ni-P substrates coated with electrodeposited Au-Cu were measured (original data) and computed.

1. Introduction

Crack arrest fracture toughness K_{Ic0} (i.e. a particular kind of toughness, which is conceptually different from the current fracture mechanics toughness K_{Ic}, as correctly stressed by [1–3]) can be evaluated for thick supported films as described in a previous paper by the authors of this research [4]. In that paper an extrapolation procedure was proposed for metallic coatings, based on the traditional Palmqvist approach for bulk ceramic materials [5]; such a method proved effective with a series of metallic materials and metal-matrix composites [6–8] in which the Palmqvist cracks induced in the coating do not interfere with the coating/substrate interface. If the same procedure is applied to systems where either the crack path or the indentation geometry are affected by the substrate, the quantitative value of the K_{Ic0} estimates is doubtful and only comparative work can be based on the technique, since the parameter figures would be devoid of mechanical meaning.

In this paper a simple analytical approach is proposed for the case of thinner coatings, in which the indentation process is directly affected by the presence of the substrate.

2. The model

2.1. Definition of plasticised volumes

In the hypothesis that the film is thin with respect to the Vickers indentation diagonal, the plasticised volume (which can be treated as semi-spherical according to the inclusion core model [9]) can be considered to occupy a cylindrical portion within the film. In this case the plasticised volume V_{PF} of the film is:

$$V_{PF} = \pi r_{PF}^2 s$$

The plasticised volume under a Vickers indentation can be treated with the following conceptual tools: (i) inclusion core model [9], (ii) modification of the plasticised volumes due to adhesive coupling of the coating to the substrate (original elaborations of results presented in [10]). The plasticised volume within the substrate can be assumed to have the shape of a spherical domes of radius r_{PS}, being r_{PS} a function of a_{PS} and b_{PS} (see Fig. 1); the following limiting relation hold: $r_{PF} \leq r_{PS} < \infty$, which corresponds to: $0 \leq a_{PS} \leq r_{PF}$. It follows that:

$$V_{PS} = \frac{4}{4}\pi\left(\frac{a_{PS}}{2}\right)^3 + \pi b_{PS}\frac{a_{PS}}{2} = \frac{\pi}{3}a_{PS}^2(3r_{PS} - a_{PS})$$

Elaborating on [10], the following relationship can be established between V_{PF} and V_{PS}:

$$\chi^3 = \frac{V_{PF}(H_F - H_C)}{V_{PS}(H_C - H_S)}$$

where χ is the an adhesion parameter and H denotes hardness (the subscripts C, F and S stand for: coating,

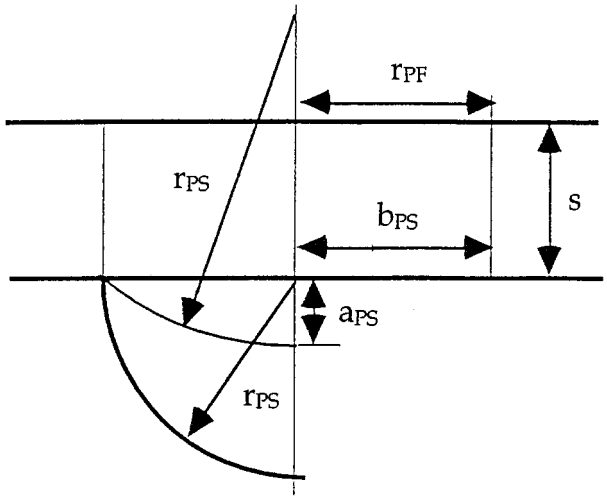

Figure 1 Definition of the symbols used in Section 2.1.

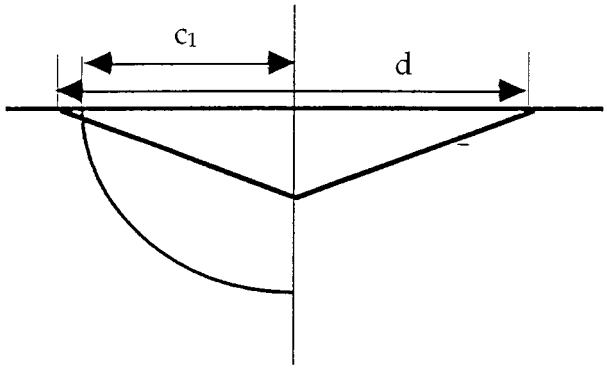

Figure 2 Definition of the symbols used in Section 2.2.

film and substrate, respectively). The upper limiting value of the adhesion parameter (faultless interface) χ can be related to the Young's modulus E and the hardness of film and substrate as:

$$\chi \leq \left(\frac{E_F H_S}{E_S H_F}\right)^{\frac{1}{2}\div\frac{1}{3}}$$

2.2. Estimating r_{PF}

In this model we assume that $s \ll c_1$ (see Fig. 2); if this hypothesis does not hold, the thick film approach [4] can be used. From the inclusion core model [9]: $r_{PF} \cong c_1 \cong 0.40d$, therefore

$$V_{PF} = \pi r_{PF}^2 s = 0.16\pi d^2 s$$

and

$$V_{PS} = \frac{V_{PF}}{\chi}\frac{H_F - H_C}{H_C - H_S}$$

The latter relation defines the quantity a_{PS} through the transcendental equation:

$$V_{PS} = \frac{\pi}{6}a_{PS}^3 + 0.08\pi d^2 a_{PS}$$

2.3. Stress distributions in the film and substrate

In this approach the stress evaluations in the film and substrate are decoupled. The stress transmission through the film/substrate interface is accounted for through the adhesion parameter χ. The stress state of the film is not affected by the nature of the substrate, provided the latter can support the former, forming a mechanical continuum. On the contrary, the stress state of the substrate depends on the mechanical properties of the film, since the load transmission is affected by it.

2.3.1. Stress distribution in the film

From the inclusion core model:

$$\sigma_F^\infty(r) = -\frac{P}{0.16\pi d^2} \quad \text{for} \quad r < r_{PF}$$

$$\sigma_F^\infty(r) = \sigma_{SF}\left(\frac{1}{3} - 2\ln\frac{b_F}{r}\right) \quad \text{for} \quad r_{PF} \leq r \leq b_F$$

$$\sigma_F^\infty(r) = \frac{\sigma_{SF}}{3}\left(\frac{b_F}{r}\right)^3 \quad \text{for} \quad r > b_F$$

where P is the load and b_F is defined - for the case of a Vickers indenter - by:

$$b_F^3 \cong 5.32 d^3 \frac{E_F}{\sigma_{SF}}(1 - \upsilon_F)$$

2.3.2. Stress distribution in the substrate

The quantity h (see Fig. 3) is defined as:

$$h = \sqrt{\left(\frac{a_{PS}}{2}\right)^3 + \frac{3}{8}r_{PF}^2 a_{PS}} - s - a_{PS}$$

and r can be expressed as a function of ρ and θ as:

$$r^2 = (h + s + \rho\cos\theta)^2 + \rho^2 \sin^2\theta$$

It follows that:

$$\sigma_S^\infty(r) = -\frac{P}{0.16\pi d^2} \quad \text{for} \quad r < s + a_{PS} + h$$

$$\sigma_S^\infty(r) = \sigma_{SS}\left(\frac{1}{3} - 2\ln\frac{b_S}{r}\right)$$

$$\text{for} \quad h + s + a_{PS} \leq r \leq b_S$$

$$\sigma_S^\infty(r) = \frac{\sigma_{SS}}{3}\left(\frac{b_S}{r}\right)^3 \quad \text{for} \quad r > b_S$$

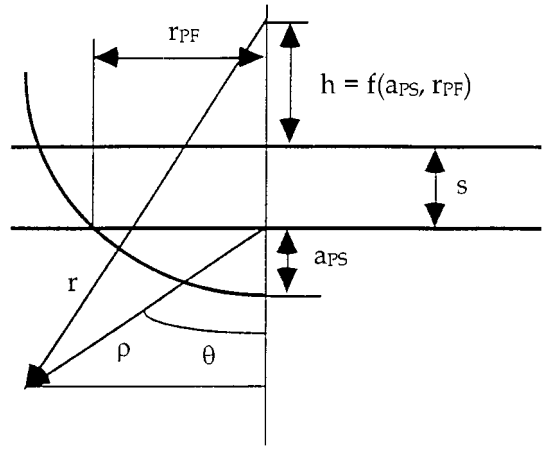

Figure 3 Definition of the symbols used in Section 2.3.2.

with b_S defined - for the case of a Vickers indeter - by:

$$b_S^3 \cong 5.32 d^3 \frac{E_S}{\sigma_{SS}}(1 - v_S)$$

2.3.3. Image stresses and local stresses

Image stresses $\sigma^{im}(r)$ must be considered in order to account for the existence of the free surface of the film. According to [9] the image stresses can be written as:

$$\sigma^{im}(r) = \int_0^\infty \sigma^\infty(\rho) f\left(\frac{r}{\rho}\right) \frac{1}{\pi\rho} d\rho$$

where:

$$f\left(\frac{r}{\rho}\right) = -\frac{5}{2}\left(\frac{r}{\rho}\right) + \frac{51}{16}\left(\frac{r}{\rho}\right)^3 - \frac{153}{64}\left(\frac{r}{\rho}\right)^5 \quad \text{for} \quad r/\rho \leq 1$$

$$f\left(\frac{r}{\rho}\right) = -\left(\frac{\rho}{r}\right)^3 - 2.5\left(\frac{\rho}{r}\right)^4 - 0.5\left(\frac{\rho}{r}\right)^5 + 6\left(\frac{\rho}{r}\right)^6 - 6.6\left(\frac{\rho}{r}\right)^7 \quad \text{for} \quad r/\rho > 1$$

The local stress is therefore defined as:

$$\sigma(r) = \sigma^\infty(r) + \sigma^{im}(r)$$

2.4. Estimating K_{Ic0} for film and substrate

Assuming that the Palmqvist crack can be approximated by a semi-elliptical one [11] and elaborating on the theory for the stress intensity factor for a halfpenny crack with a stress gradient [12]:

$$K_{Ic} = 2.24\sqrt{\frac{\pi}{2}}\bar{\sigma}\frac{m}{\sqrt{l}}$$

where:

$$\bar{\sigma} = \frac{1}{L_{CF}} \int \sigma(r)\, dr$$

The line integral must be computed along the crack front CF whose length is L. Some typical cases are discussed below.

2.4.1. Case 1: Crack depth < substrate thickness

In this case we assume that the Palmqvist-crack shape is semi-elliptical. The integral along the crack front consists in computing it along the semi-elliptical crack:

$$\bar{\sigma} = \int_0^\pi \sigma(r(\theta))\, d\theta$$

where (see Fig. 4)

$$r(\theta) = \frac{d}{2} + \frac{l}{2} - \frac{m\cos\theta}{\sqrt{1 - \left(1 - \frac{4m^2}{l^2}\right)\cos^2\theta}}$$

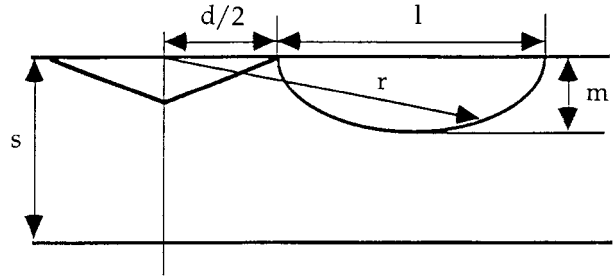

Figure 4 Definition of the symbols used in Section 2.4.1.

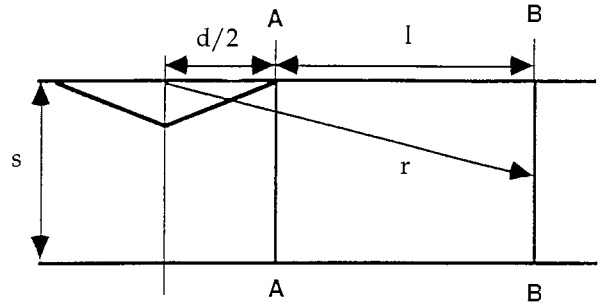

Figure 5 Definition of the symbols used in Section 2.4.2.

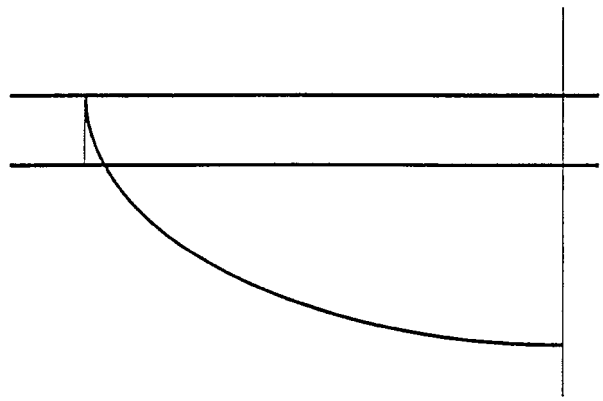

Figure 6 Approximating the portion of a semi-elliptical crack in the film by a straight line perpendicular to the film surface.

2.4.2. Case 2: Crack depth ≥ substrate thickness

In this case we assume that the crack is rectangular (see Fig. 5). In the case of a crack crossing the interface, the film material does not contribute to the crack arrest and the interfacial side of the crack front is disregarded in the computation of fracture toughness. If the crack is stopped at the interface, we can assume that the crack arrest is due to the substrate material and the same computational procedure for the estimation of the film fracture toughness can be applied as in the case of a passing crack.

For the computation of K_{Ic0} we use the same formalism as for the semi-elliptical crack, with the approximation that the sides AA and BB of Fig. 5 are linear, i.e. the upper portions of the semi-ellipsis of Fig. 6, cut by the film/substrate interface, can be considered to be so small as to be confused with straight lines perpendicular to the film surface.

The integrations required in this case are:

$$\bar{\sigma} = \int_{AA} \sigma(r(x_A))\,dx_A + \int_{BB} \sigma(r(x_B))\,dx_B$$

$$= \int_0^S \sigma(r(x_A))\,dx_A + \int_0^S \sigma(r(x_B))\,dx_B$$

with

$$r(x_A) = \sqrt{x_A^2 + \left(\frac{d}{2}\right)^2}$$

$$r(x_B) = \sqrt{x_B^2 + \left(\frac{d}{2} + l\right)^2}$$

2.4.3. Case 3: A crack in the substrate

The existence of a crack in the substrate can be used to estimate the fracture toughness of the substrate material. The crack in the film can be treated as discussed in Sections 2.4.1 and 2.4.2. The stress state in the substrate can be approximated by the sum of the stress state caused by the indentations in both the film and the substrate. The contribution to the average stress due to the indentation of the substrate can be computed as in Section 2.4.1, using the diagonal of the interfacial trace of the indentation d_i. (see Fig. 7) The contribution to the stress state caused by indentation of the film will be described in the rest of this section. The integration along the crack front is performed along the semi-ellipsis within the substrate material, by using the following transformations:

$$\rho^2(\theta) = \frac{1}{1 - \frac{\sqrt{(l/2)^4 - n^2}}{l/2}\cos^2\theta}$$

$$x(\theta) = \frac{d}{2} + \frac{l}{2} - \rho\cos\theta$$

$$y(\theta) = h + s + \rho\sin\theta$$

$$r(\theta) = \sqrt{x(\theta)^2 + y(\theta)^2}$$

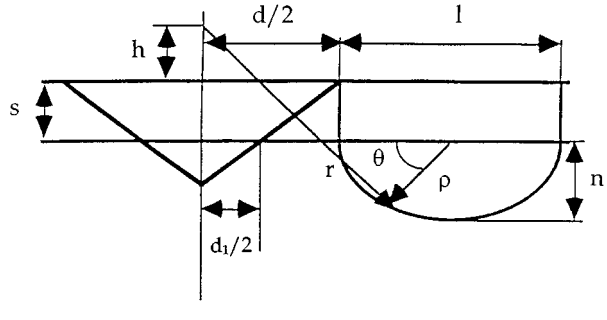

Figure 7 Definition of the symbols used in Section 2.4.3.

3. Comparison with experimental data

3.1. Materials and methods

Electroless Ni-P (9%) layers of various thicknesses were plated onto nitriding steel in the same way as reported in [4]. Au-Cu (25%) top layers were deposited from the cyanide bath described in [13] at current density = 5 mA/cm^2 and $T = 40^\circ$C. Detailed studies of the above mentioned materials are given in the following references: bath behaviour (Ni-P [14], Au-Cu [13]), deposit structure (Ni-P [15–17], Au-Cu [18]) and mechanical properties (Ni-P [19], Au-Cu [20]). The indentation procedure is the same as described in detail in [4]. The problem of the presence of an experimental residual stress state was not accounted for in the evaluation of the fracture toughness of films. We maintain that this approach is acceptable, and even advantageous, in the case at hand because the formation of residual stresses is intrinisic of the relevant film growth processes. The proposed indentation method has the advantage of quantifying with a single parameter (crack-arrest fracture toughness) both material properties and growth-induced stress states. These two quantities cannot be separated in the case of deposited films and they must be jointly taken into account as far as practical applications of the relevant coatings are concerned. This is at variance with the case of bulk metarials, where the stress states induced by the preparation technique of the measurement (e.g. metallographic polishing) - not of the material preparation process - induces errors in the evaluation of the bulk metarial fracture toughness.

3.2. Mechanical data for computations

The mechanical constants which are needed for the model computations (see Section 2) were derived from papers published previously by one of the authors (see References contained in Section 3.1).

3.2.1. Crystallised electroless Ni-P (9%)

Young's modulus: $E = 184000$ MPa
Yield stress: $\sigma_Y = 151$ MPa
Poisson's coefficient: $v = 0.30$

3.2.2. Electrodeposited Au-Cu (25%)

Young's modulus: $E = 41160$ MPa
Yield stress: $\sigma_Y = 123$ MPa
Poisson's coefficient: $v = 0.30$

3.3. Interpretation of literature data

Crack arrest fracture toughness data for relatively thick supported Ni-P layers, for which the present approach is not necessary, were published previously by the authors of the present paper [4]. These data were re-interpreted according to the model described in Section 2; this application can be considered as a limiting-case test of the model, which was designed for thinner coatings in which the interactions of the indenter with the substrate

are significant. K_{Ic0} estimates as a function of applied load are reported in Fig. 8 for both the thick-film [4] and the thin-film (Section 2) approaches. The two sets of evaluations are comparable and yield results which are both quite acceptable interpretations of the experimental data, taking into account their spread.

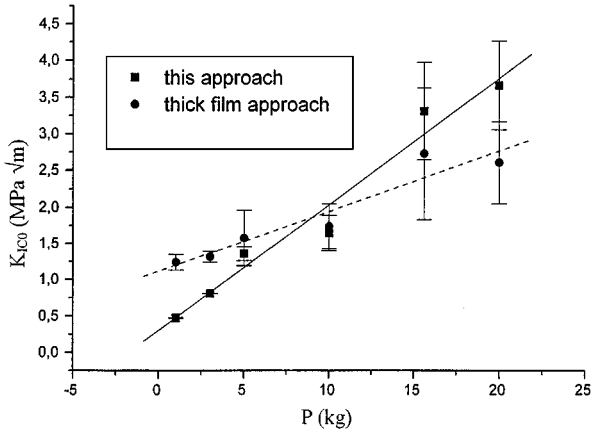

Figure 8 Crack arrest fracture toughness (K_{Ic0}) estimates as a function of indentation load according to the thick-film [3] and thin-film (Section 2) approaches.

3.4. Ni-P coatings of various thicknesses

Ni-P coatings in three thickness ranges were plated onto nitriding steel, heat treated and indented with different loads. Experimental conditions, indentation diagonals and crack lengths are reported in Table I. The average crack lengths and standard deviations were computed from the average crack lengths of the four angular cracks (see Fig. 9) of each replicated measurement.

K_{Ic0} estimates were computed with the model proposed in Section 2 and are reported in Table II. Upper and lower limits for K_{Ic0} estimates were evaluated by computing the crack arrest fracture toughness with the following input values: $(\langle d\rangle - \sigma_d, \langle l\rangle + \sigma_l)$ and $(\langle d\rangle + \sigma_d, \langle l\rangle - \sigma_l)$, respectively. The relevant analytical expressions of Section 2 were integrated numerically with optimal integration parameters.

The K_{Ic0} estimates agree well with the values previously reported [4] for thick films, supporting the thesis that the parameter is a material property. No trends can be observed in the investigated ranges of thicknesses and indentation loads, the estimated crack arrest fracture toughness K_{Ic0} amounts to $1.09\,\mathrm{MPa}\sqrt{\mathrm{m}}$, the spread of the estimates is in the range: $0.80 \div 1.41\,\mathrm{MPa}\sqrt{\mathrm{m}}$.

3.5. Thin Au-Cu coatings on thick Ni-P

A disordered Au-Cu (25%) film of thickness 2 μm (evaluated from a SEM cross section) was electroplated

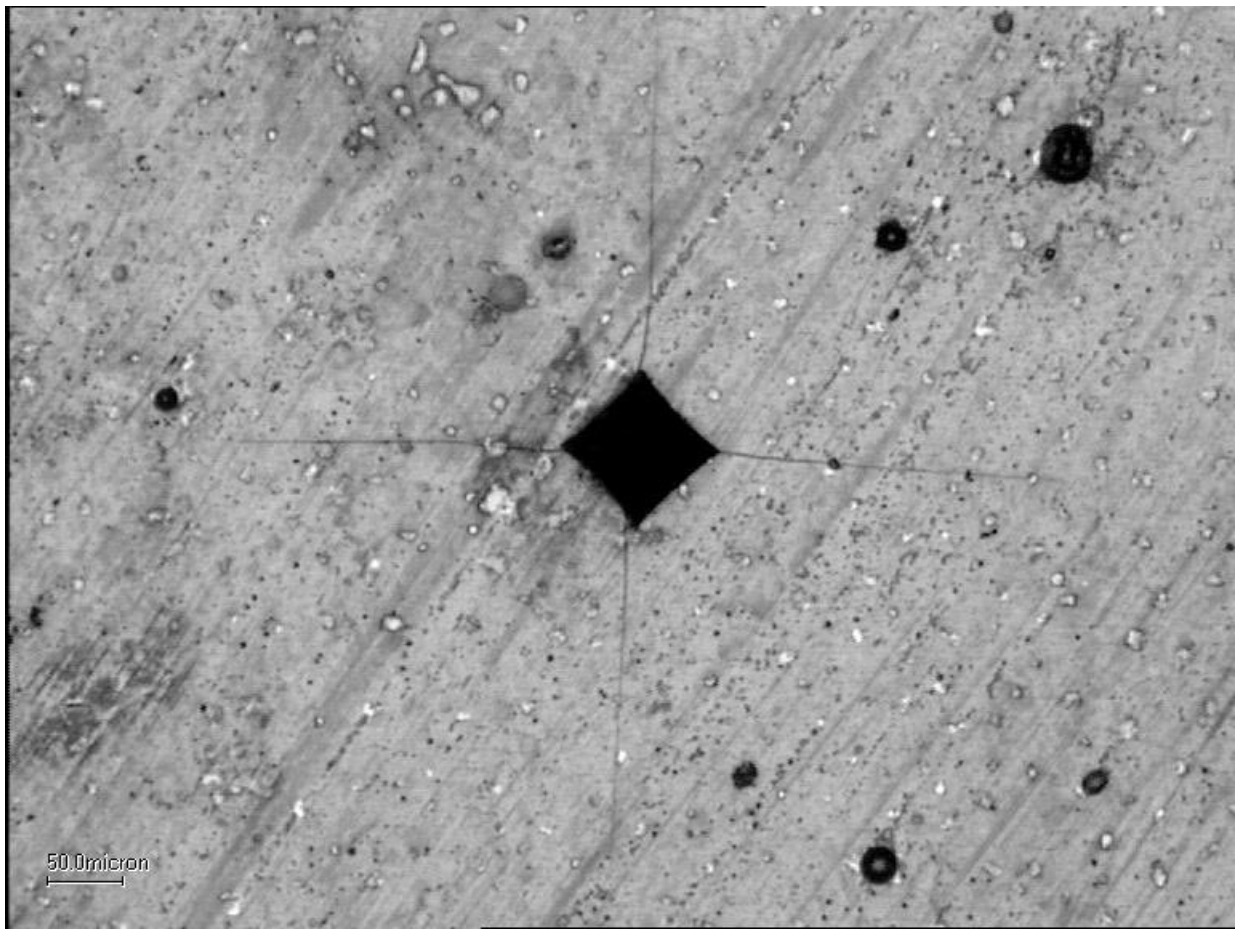

Figure 9 Optical micrograph of Vickers indentation (sample thickness: 5 μm, indentation load. 3 kg) and relevant angular cracks.

TABLE I Crystalline Ni-P (9%) films: thicknesses s, indentation loads P, indentation diagonals d and crack lengths l

	$P=1$ kg	$P=3$ kg	$P=5$ kg
$s=5$ μm	$d=72.13\pm4.25$ μm	$d=110.75\pm6.76$ μm	$d=167.93\pm8.19$ μm
	$l=61.16\pm6.89$ μm	$l=230.03\pm6.05$ μm	$l=223.3\pm7.96$ μm
$s=10$ μm	$d=68.00\pm3.97$ μm	$d=123.60\pm4.45$ μm	$d=162.30\pm8.00$ μm
	$l=65.60\pm4.25$ μm	$l=142.03\pm10.15$ μm	$l=190.83\pm9.60$ μm
$s=17.5$ μm	$d=62.91\pm5.41$ μm	$d=116.97\pm6.10$ μm	$d=154.30\pm9.34$ μm
	$l=51.40\pm5.31$ μm	$l=108.50\pm5.26$ μm	$l=184.13\pm6.76$ μm

TABLE II Crack arrest fracture toughness K_{Ic0} estimates (MPa$\sqrt{}$m) and upper K_{upp} and lower K_{low} limits computed with the model of Section 2 as a function of film thickness s and indentation load P

	$P=1$ kg	$P=3$ kg	$P=5$ kg
$s=5$ μm	$K_{low}=0.94$	$K_{low}=1.08$	$K_{low}=1.14$
	$K_{Ic0}=1.07$	$K_{Ic0}=1.11$	$K_{Ic0}=1.17$
	$K_{upp}=1.23$	$K_{upp}=1.13$	$K_{upp}=1.19$
$s=10$ μm	$K_{low}=0.88$	$K_{low}=0.85$	$K_{low}=0.95$
	$K_{Ic0}=1.06$	$K_{Ic0}=0.98$	$K_{Ic0}=1.09$
	$K_{upp}=1.28$	$K_{upp}=1.13$	$K_{upp}=1.25$
$s=17.5$ μm	$K_{low}=0.80$	$K_{low}=1.06$	$K_{low}=0.91$
	$K_{Ic0}=1.04$	$K_{Ic0}=1.22$	$K_{Ic0}=1.05$
	$K_{upp}=1.37$	$K_{upp}=1.41$	$K_{upp}=1.20$

onto thick ($\sim$70 μm) as plated and mechanically polished electroless Ni-P deposited onto nitriding steel. The sample was indented with a load of 5 kg. Experimental surface and interface indentation diagonals and crack lengths are shown in Figs 10–12. The results of crack arrest fracture toughness evaluations according to the procedure described in Section 2.4.3 are: K_{Ic0}(Au-Cu) = 1.25 MPa$\sqrt{}$m, K_{low}(Au-Cu) = 1.21 MPa$\sqrt{}$m, K_{upp}(Au-Cu) = 1.31 MPa$\sqrt{}$m; this figure is in slight excess of the values measured in a different paper [21], where the value $K_{Ic0}=0.89$ MPa$\sqrt{}$m was obtained for thicker ($\sim$40 μm) layers indented with a micro-Vickers indenter loaded with 0.5 kg and evaluated with the thick-film method [4].

The model of Section 2 was used to estimate the K_{Ic0} for the X-ray amorphous Ni-P substrate into which the crack was propagated through the interface. The interfacial crack length and the interfacial diagonal were measured by the lapping method described in [4], the results are: K_{Ic0}(Ni-P) = 4.48 MPa$\sqrt{}$m, K_{low}(Ni-P) = 3.84 MPa$\sqrt{}$m, K_{upp}(Ni-P) = 5.34 MPa$\sqrt{}$m, these

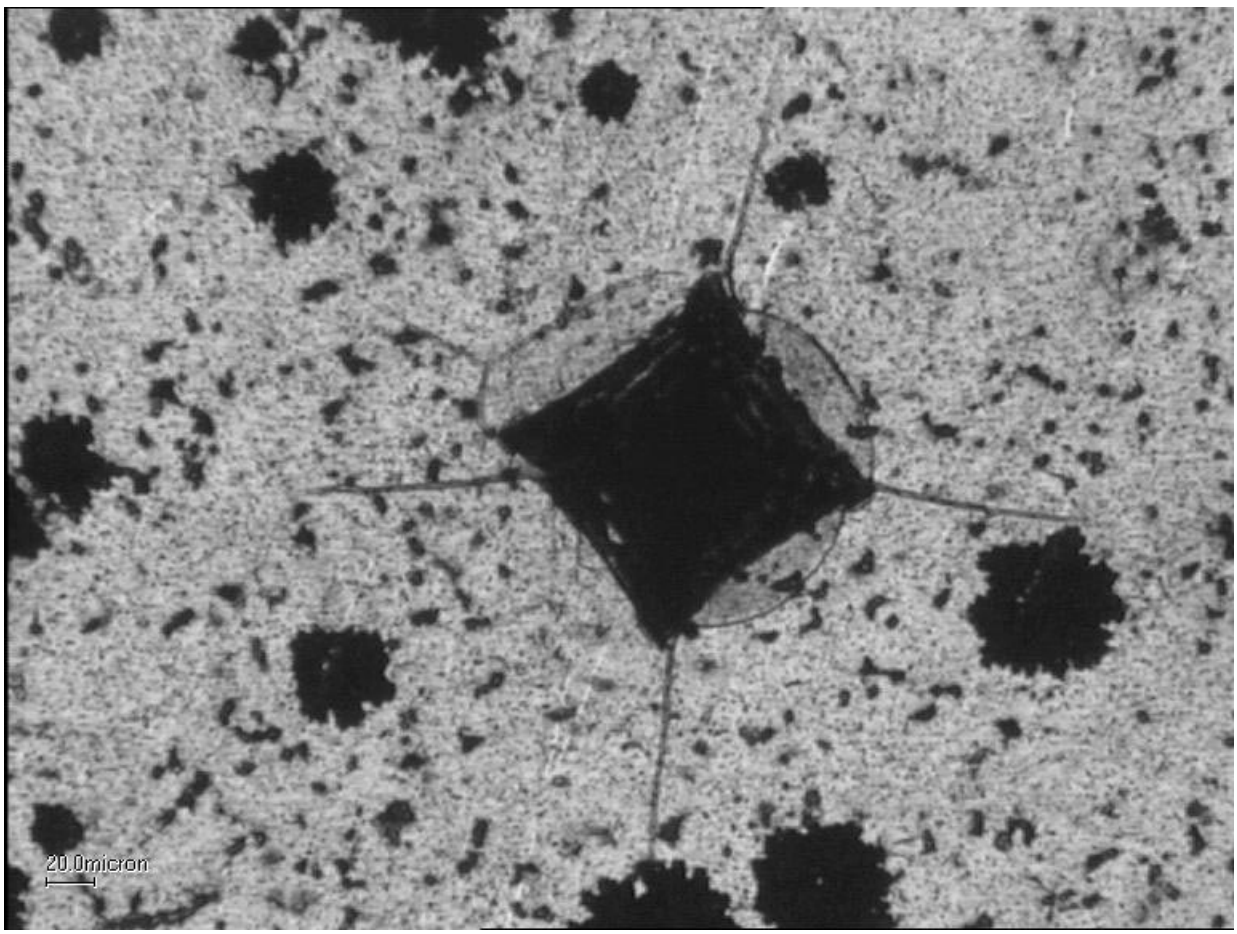

Figure 10 SEM micrograph of the surface Vickers indentation and crack system of a 2 μm Au-Cu film deposited onto an amorphous Ni-P substrate ($\sim$70 μm).

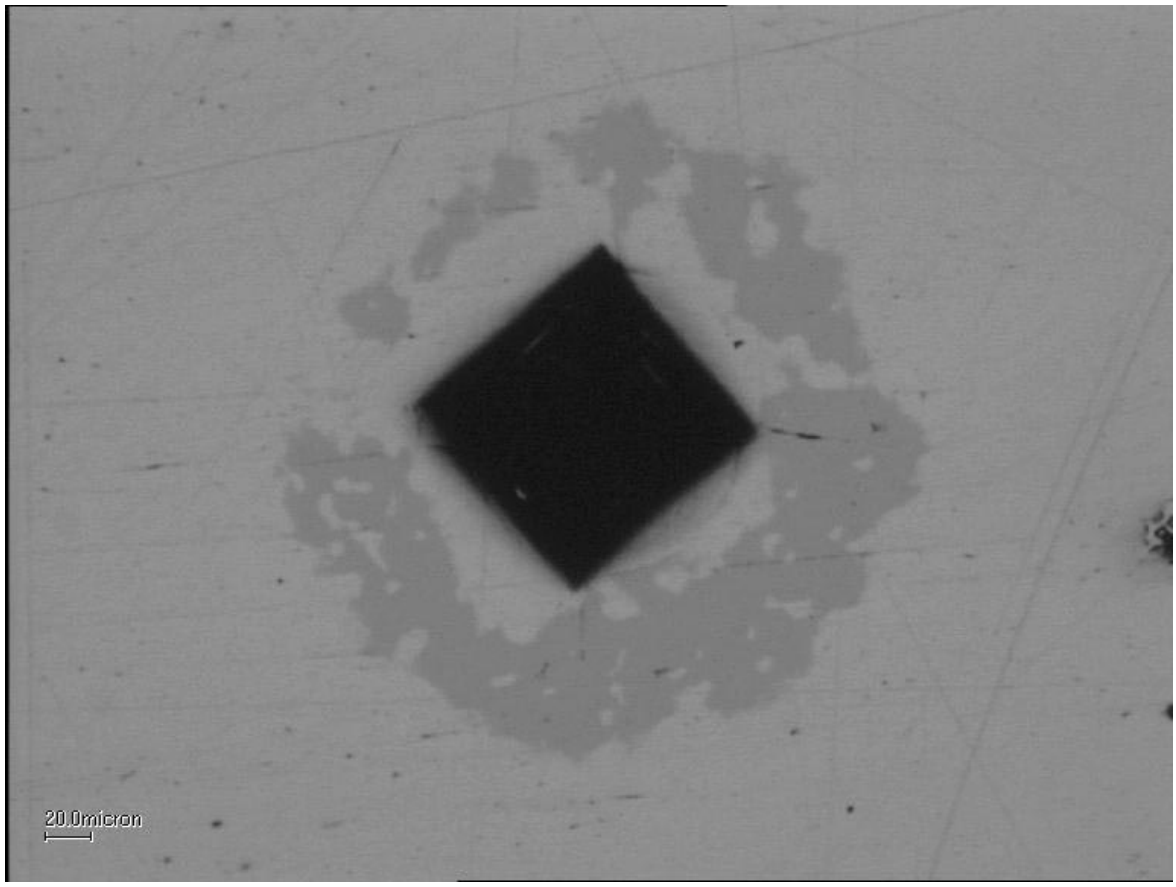

Figure 11 SEM micrograph of the trace of a Vickers indentation at the Au-Cu/Ni-P interface (see Fig. 10).

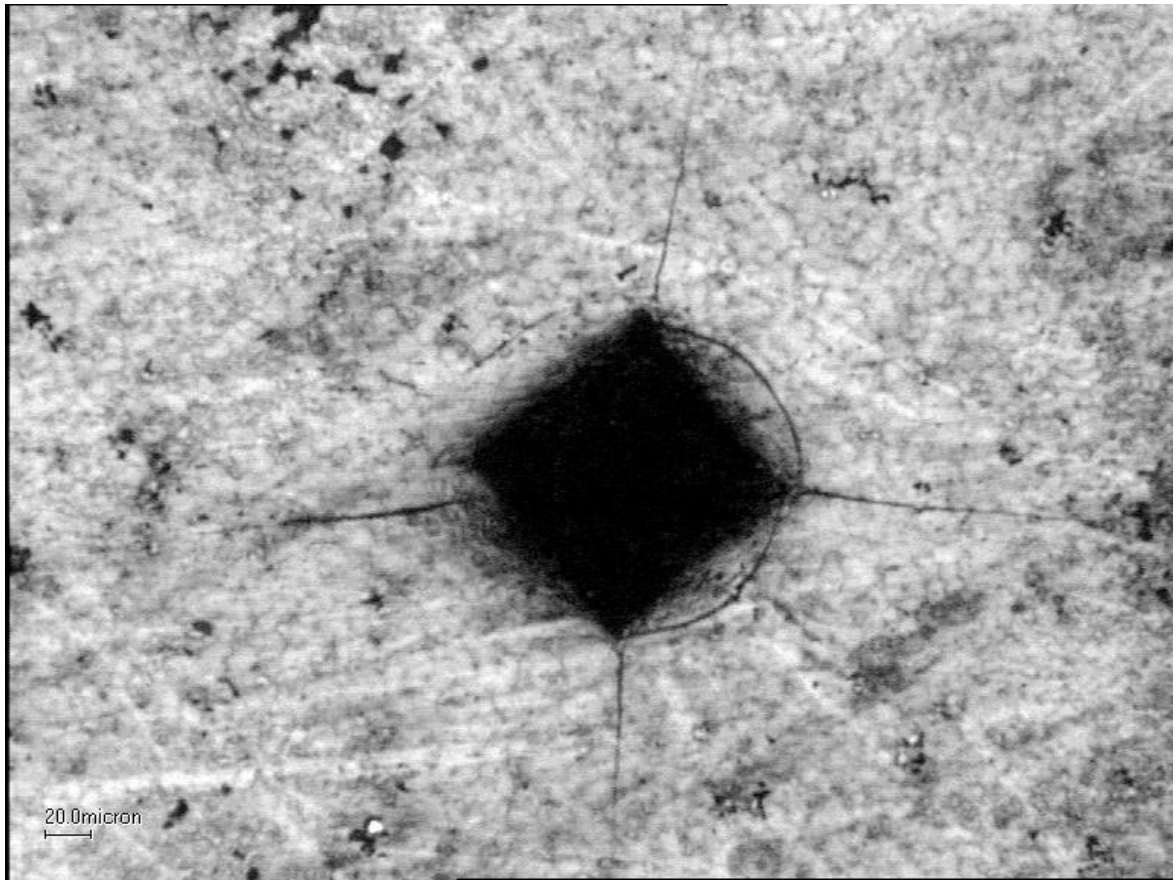

Figure 12 SEM micrograph of the interfacial trace of a Vickers indentation and of the interfacial crack system in the Ni-P substrate of a Au-Cu/Ni-P bilayer (see Fig. 10).

results underestimate the results reported in [4], but are still in fair agreement.

4. Conclusions

In this paper, a simple analytical model is proposed for the measurement of crack arrest fracture toughness of thin supported films by Vickers indentation. In this context by "thin film" we mean a system in which the indentation process is directly affected by the presence of the substrate, i.e. the indentation depth is larger than the film thickness and/or a Palmqvist crack crosses the film/substrate interface.

The model is based on the following mechanical-metallurgical concepts: (i) plasticised volume under a Vickers indentation, treated with the inclusion core model [9]; (ii) modification of the plasticised volumes due to adhesive coupling of the coating/substrate system, treated according to [10]; (iii) modelling of Palmqvist cracks by semielliptical cracks, obtained by elaborating on [11].

Analytical expressions are given for the crack arrest fracture toughness as a function of: (i) mechanical parameters of film and substrate (Young's modulus, yield strength, Poisson coefficient), (ii) geometry of the system (film thickness, indentation diagonal, crack length, crack depth) and (iii) interfacial adhesion (which can be either measured or estimated from mechanical properties of the film and substrate for the case of ideally fault-free interfaces). The derived analytical expressions cannot really be handled analytically, but can be solved by straightforward numerical integration. The model was tested against three sets of experimental data: (i) literature crack arrest fracture toughness K_{Ic0} data for thick Ni-P films were re-evaluated by this model as a limiting case test: a good agreement was found; (ii) Ni-P coatings of various thicknesses were tested with different indentation loads in a system where the cracks were either shallower than the film or were arrested at the Ni-P/steel interface and K_{Ic0} values were obtained which were consistent both among themselves and with the results of point (i); (iii) thin Au-Cu coatings plated onto Ni-P substrates were produced and tested: in this system the crack propagates though the interface and K_{Ic0} of both coating and substrate can be evaluated: a fair consistency of the estimates of Ni-P and Au-Cu crack arrest fracture toughness values was found.

References

1. M. SAKAI and R. C. BRADT, *Internat. Materials Rev.* **38** (1993) 53.
2. R. MORRELL, CEN/TC: 184/WG3/N/68 10/11/1992.
3. R. J. PRIMAS and R. GSTREIN, *Fatigue Fract. Engng. Mater. Struct.* **20** (1997) 513.
4. B. BOZZINI and M. BONIARDI, *Z. f. Metallkunde* **88** (1997) 493.
5. C. B. PONTON and R. D. RAWLINGS, *Mat. Sci. Technol.* **5** (1989) 865.
6. B. BOZZINI, A. BROTZU, M. CECCHINI, G. GIOVANNELLI, S. NATALI, P. L. CAVALLOTTI, G. SIGNORELLI and B. BREVAGLIERI, in Proc. 11th IFHT, 4th ASM, Florence (I), 19, 21/10/1998.
7. B. BOZZINI, M. BONIARDI and P. L. CAVALLOTTI, Atti 13° Conv. Naz. G.I.F., edited by N. Bonora and F. Iacoviello, Cassino (I) (1997) p. 137.
8. B. BOZZINI, G. GIOVANNELLI, M. BONIARDI and P. L. CAVALLOTTI, in Proc. 11th IFHT, 4th ASM, Florence (I), 19, 21/10/1998.
9. K. TANAKA. *J. Mater. Sci.* **22** (1987) 1501.
10. S. J. BULL and D. S. RICKERBY, *Surf. and Coat. Technol.* **42** (1990) 149.
11. K. NIIHARA, *J. Mater. Sci. Lett.* **2** (1983) 221.
12. K. TANAKA, *Scripta Metall.* **19** (1985) 1183.
13. B. BOZZINI, G. GIOVANNELLI and P. L. CAVALLOTTI, *J. Appl. Electrochem.* **29** (1999) 685.
14. P. L. CAVALLOTTI and B. BOZZINI, in "Neue Werkstoffe und Technologien in der Oberflächentechnik zur Verbesserung des Korrosions- und Tribologieverhaltens," edited by A. Choms (E. G. Leuze Vlg., Saulgau Württ., 1994) p. 91.
15. B. BOZZINI and P. L. CAVALLOTTI, *Scripta Mater.* **36** (1997) 1245.
16. B. BOZZINI, N. LECIS and P. L. CAVALLOTTI, *J. Phys. IV France* **8** (1998) 2.
17. B. BOZZINI, P. L. CAVALLOTTI and G. GIOVANNELLI, *La metallurgia italiana* **90** (1998) 35.
18. B. BOZZINI, P. L. CAVALLOTTI, G. GIOVANNELLI, B. BREVAGLIERI, S. NATALI and G. SIGNORELLI, in "Atti Convegno FAST: Materiali," Milan (I) (1997) Vol. 2, p. 875.
19. M. BONIARDI, B. BOZZINI, G. C. MARTINELLI and R. VITALI, *Int. J: Material and Product Technology* **15** (2000) 63.
20. B. BOZZINI, P. L. CAVALLOTTI, G. GIOVANNELLI, B. BREVAGLIERI, S. NATALI and G. SIGNORELLI, in "Atti Convegno FAST: Materiali," Milan (I) (1997) Vol. 2, p. 883.
21. B. BOZZINI, G. GIOVANNELLI, S. NATALI, B. BREVAGLIERI, P. L. CAVALLOTTI and G. SIGNORELLI, *Eng. Fail. Anal.* **6** (1999) 83.

Received 25 February 1999
and accepted 19 January 2000